Mechanism of Transfer of LDL-Derived Free Cholesterol to HDL Subfractions in Human Plasma†

T. Miida, C. J. Fielding, and P. E. Fielding*
Cardiovascular Research Institute and Departments of Medicine and Physiology, University of California, San Francisco, San Francisco, California 94143

Received May 2, 1990; Revised Manuscript Received August 1, 1990

ABSTRACT: The transfer of [^{3}H]cholesterol in low-density lipoprotein (LDL) to different high-density lipoprotein (HDL) species in native human plasma was determined by using nondenaturing two-dimensional electrophoresis. Transfer from LDL had a $t_{1/2}$ at 37 °C of 51 ± 8 min and an activation energy of 18.0 kCal mol^{-1}. There was unexpected specificity among HDL species as acceptors of LDL-derived labeled cholesterol. The largest fraction of the major α-migrating class (HDL_{2b}) was the major initial acceptor of LDL-derived cholesterol. Kinetic analysis indicated a rapid secondary transfer from HDL_{2b} to smaller αHDL (particularly HDL_3) driven enzymatically by the lecithin–cholesterol acyltransferase reaction. Rates of transfer among αHDL were most rapid from the largest αHDL fraction (HDL_{2b}), suggesting possible protein-mediated facilitation. Simultaneous measurements of the transport of LDL-derived and cell-derived isotopic cholesterol indicated that the former preferably utilized the αHDL pathway, with little label in pre-βHDL. The same experiments confirmed earlier data [Castro, G. R., & Fielding, C. J. (1988) *Biochemistry 27*, 25–29] that cell-derived cholesterol is preferentially channeled through pre-βHDL. We suggest that the functional heterogeneity of HDL demonstrated here includes the ability to independently process cell- and LDL-derived free cholesterol.

Free cholesterol from both peripheral cell membranes and secreted lipoproteins can be utilized as substrate for the lecithin–cholesterol acyltransferase (LCAT) reaction in human plasma. These substrates contribute to the reaction sequence ("reverse cholesterol transport") which returns extrahepatic cholesterol to the liver for degradation (Fielding, 1990). Recent research from this laboratory has focused on the pathway by which free cholesterol removed from cell membranes appears as cholesteryl ester in the circulation. Three pre-β-migrating high-density lipoprotein (HDL) species have been identified which appear to play key roles in the early metabolic handling of cell-derived cholesterol (Castro & Fielding, 1988; Francone et al., 1989). These studies, however, did not determine whether lipoprotein cholesterol, also esterified by LCAT, utilizes the same intermediates or whether cell- and lipoprotein-derived free cholesterol are distinguished in the early metabolism of cholesterol in plasma.

Quantitatively, the most important lipoprotein donor of free cholesterol to the LCAT reaction is low-density lipoprotein (LDL) (Fielding & Fielding, 1981a; Park et al., 1987). In the present experiments, the mechanism of transfer of LDL free cholesterol to other lipoprotein complexes in native plasma has been investigated. The kinetics of cell-derived and LDL-derived cholesterol in plasma have been compared. The results indicate that cell-derived and LDL-derived cholesterol are largely metabolized by separate pathways in plasma and that a high molecular weight αHDL fraction (HDL_{2b}) plays the major role in the early processing of free cholesterol from LDL.

Experimental Procedures

Blood was obtained from healthy normolipidemic volunteers who had fasted overnight. The blood was taken into ice-cooled plastic tubes containing 5 μg/mL D-phenylalanyl-L-prolyl-L-arginyl chloromethyl ketone or 150 units/mL streptokinase as anticoagulant for subsequent incubation with cell monolayers (Castro & Fielding, 1988). Plasma was obtained by centrifugation (2000*g*, 30 min, 0 °C) and used immediately in the experiments described below.

Preparation of [^{3}H]Cholesterol-Labeled LDL. LDL was rapidly purified from plasma by affinity chromatography. Plasma (8 mL) was added to a column (2 × 20 mL) of heparin–agarose (Pharmacia-LKB, Piscataway, NJ) equilibrated in 0.15 M NaCl–0.01% EDTA, pH 7.4. Lipoproteins retained by the column [LDL and very low density lipoprotein (VLDL) containing apo E (Fielding & Fielding, 1987)] were eluted with 3 M NaCl, 10 mM Tris-HCl, pH 7.4, and 0.01% EDTA. The eluate was immediately fractionated on a column of agarose covalently complexed with rabbit anti-human apo E IgG (Porath et al., 1972) to remove VLDL containing apo E, and the unretained fraction containing LDL was collected.

LDL prepared as above was labeled by equilibration with [^{3}H]cholesterol–albumin–agarose complex. Human recrystallized albumin (Sigma, St. Louis, MO) was covalently complexed to agarose beads (Affi-Gel, Bio-Rad, Richmond, CA) according to the manufacturer's instructions. The protein–bead complex formed was washed with 20 volumes of 0.15 M NaCl–10 mM Tris-HCl, pH 7.4. The complex was then labeled by incubation at 37 °C for 60 min with 0.5–1.0 mCi of [1,2-^{3}H]cholesterol (NEN, Boston, MA) (50–60 Ci/mmol) dissolved in 20 μL of ethanol. After incubation, the agarose–albumin complex was collected by centrifugation at 0 °C for 30 s at 800 rpm. The supernatant was removed and the complex washed 3 times as above with 0.15 M NaCl–10 mM Tris-HCl, pH 7.4. Affinity-purified LDL was then added to the [^{3}H]cholesterol-labeled agarose–albumin complex. The mixture was incubated with gentle stirring at 37 °C for 60 min to allow equilibration of the [^{3}H]cholesterol between albumin and LDL. The beads were then removed by brief low-speed centrifugation, and the labeled LDL in the supernatant was recovered. The specific activity of free cholesterol in the labeled LDL was between 1.8 × 10^7 and 2.6 × 10^7 cpm/μg. LDL labeled in this way comigrated with plasma

†This research was supported by National Institutes of Health through Arteriosclerosis Grant SCOR HL 14237.

0006-2960/90/0429-10469$02.50/0

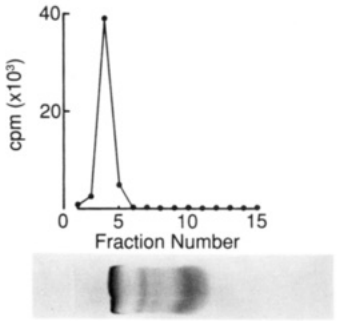

FIGURE 1: Electrophoresis of [^{3}H]cholesterol-labeled LDL purified by heparin affinity and immunoaffinity chromatography. The labeled fraction, purified as described under Experimental Procedures, was electrophoresed in agarose, at the same time as a sample of native autologous plasma. The comigration of isolated labeled LDL and the authentic LDL of native plasma is indicated.

LDL by agarose gel electrophoresis (Figure 1).

Cell Culture. As previously reported (Fielding & Fielding, 1981b; Fielding et al., 1982; Francone et al., 1989), the membrane-free cholesterol of monolayers of normal human fibroblasts or endothelial cells serves as an effective substrate for plasma LCAT activity. In the present studies, skin fibroblasts were grown in Dulbecco's modified Eagle's medium in 3.5-cm petri dishes to near-confluency (cell cholesterol, 3–4 μg/dish). To label cellular cholesterol, the cells were preincubated for 48 h in the presence of 0.5–1.0 mCi of [1,2-^{3}H]cholesterol complexed with fetal calf serum (Castro & Fielding, 1988). Cells labeled in this way show first-order cholesterol transfer rates into plasma with a $t_{1/2}$ of 10–15 h at 37 °C (Fielding & Fielding, 1981b).

For individual experiments, monolayers were washed 4 times with phosphate-buffered saline. To study the transfer and metabolism of cell-derived cholesterol, unlabeled native plasma (1 mL) was added to labeled cell monolayers. To study the transfer and metabolism of LDL-derived cholesterol, autologous unlabeled native plasma was quickly brought to the indicated temperature, labeled tracer LDL added (representing 1–2 μg of free cholesterol), and the mixture added to the unlabeled cell monolayer at the same temperature. In both cases, the plasma was brought rapidly (2–3 min) to the temperature of the experiment. Cells and plasma were incubated on an orbital shaker (1 cycle/s) during incubation at the indicated temperature. Plasma samples were taken during the incubation at times from 0.25 to 15 min in different experiments. These samples were immediately chilled in ice water and centrifuged (5 min, 4 °C, 8800*g*) to remove any particulate material. The distribution of [^{3}H]cholesterol radioactivity among lipoprotein species was then determined following one-dimensional or two-dimensional electrophoresis at 0 °C.

Nondenaturing Gel Electrophoresis. Two-dimensional electrophoresis was carried out essentially as described by Francone et al. (1989) except that in the second (gradient) dimension, separation was increased from 12.5 to 15.0 cm to increase the separation of the α-migrating HDL species. Following electrophoresis, half of the gel was used for transfer to nitrocellulose while the other half was kept at 4 °C. The nitrocellulose paper was then immunoblotted for apo A-I (Castro & Fielding, 1988). Rabbit polyclonal antibody to human apo A-I was purified by antigen immunoaffinity chromatography (Francone et al., 1989). The purified antibody was reacted with the separated proteins on nitrocellulose, and the reactive complexes were labeled with goat anti-rabbit ^{125}I-IgG. The autoradiograph from this blot was then used as a template to locate the corresponding lipoprotein regions in the original gel. These sections of gel were cut out and the

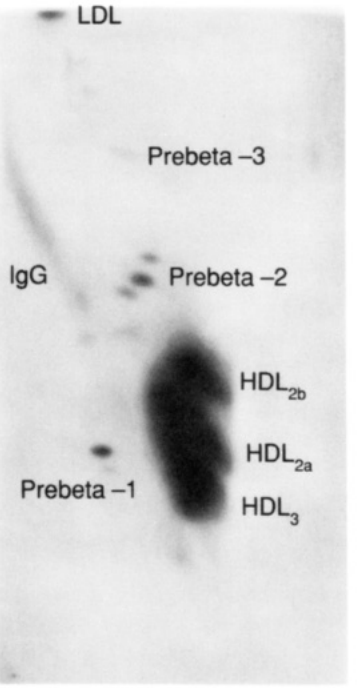

FIGURE 2: Two-dimensional nondenaturing electrophoresis of native plasma. First-dimension separation (horizontal axis) was in 0.5% agarose; second-dimension separation (vertical axis) was in a nondenaturing gradient (2–15% w/v) polyacrylamide gel (Francone et al., 1989). Following electrophoresis as described under Experimental Procedures, the separated proteins were transferred to a nitrocellulose membrane and apo A-I containing complexes identified by reaction first with polyclonal rabbit anti-human apo A-I antibody and then with ^{125}I-labeled goat anti-rabbit IgG. The distribution of reactivity is visualized following autoradiography. Pre-β-migrating HDL species are defined as previously (Francone et al., 1989). α-Migrating HDL species (HDL_{2b}, HDL_{2a}, and HDL_3) are labeled as proposed by Anderson et al. (1977, 1978).

lipoproteins eluted with 0.15 M NaCl and 0.01% EDTA, pH 7.4, containing 2.0 mM dithiobis(2-nitrobenzoic acid) (DTNB) to inhibit LCAT activity (Stokke & Norum, 1972). To determine the efficiency of extraction by this method, after elution the gel pieces were added directly to scintillation vials, the vials were tightly capped, and the gel was digested in 0.4 mL of 30% H_2O_2. No further radioactivity could be detected in the digest, indicating that the original elution procedure was essentially complete. In some experiments, free and esterified cholesterol label were fractionated by thin-layer chromatography on silica gel plates developed in hexane–diethyl ether–acetic acid, 83/16/1 v/v. Because of the short period of incubation and the rapid transfer of free cholesterol label from LDL, in the present studies esterified cholesterol represented <2% of the total label.

Nondenaturing gradient electrophoresis modified as described distinguished three species in the major (α migrating) HDL fraction (Figure 2). A similar fractionation has been reported for centrifugally isolated HDL (Anderson et al., 1977). The component electrophoretic bands were identified with centrifugal fractions HDL_{2b}, HDL_{2a}, and HDL_3 in order of increasing migration rate. Further analysis, described below, confirms this identification. However, it should be borne in mind that in the present study, the terms HDL_{2b}, HDL_{2a}, and HDL_3 refer exclusively to the α-migrating component of each size range.

Determination of Lipoprotein Diameter and Apparent Molecular Weight. Lipoprotein fractions visualized by autoradiography were excised from second-dimension nondenaturing gels developed as described above; the pieces were ap-

plied to individual channels in a 3–24% nondenaturing polyacrylamide gel and electrophoresed to equilibrium (Ishida et al., 1987) simultaneously with globular protein standards of known molecular weight and diffusion coefficient (Sigma Chemical Co., MW GF-1000 standards). The effective diameter of each standard was determined from the Stokes–Einstein equation, and the Stokes diameter (d) of each HDL fraction was determined from the observation (Rodbard et al., 1971) that ln d is inversely proportional to migration distance.

Lipid Determinations. Plasma and lipoprotein free cholesterol and triglyceride concentrations were determined by using a Roche Mira autoanalyzer. Pentuplicate determinations showed a coefficient of variance of <1%. In the present study, mean plasma total cholesterol was 155 ± 4 mg/dL plasma, plasma triglyceride was 54 ± 12 mg/dL, and HDL total cholesterol was 52 ± 12 mg/dL. Total HDL free cholesterol was determined following precipitation of LDL with dextran sulfate (0.1 mg/mL, MW 5×10^5) (Pharmacia) and magnesium chloride (0.05 M) and was 14 ± 3 mg/dL in these experiments. LDL-free cholesterol was determined following the ultracentrifugal flotation of VLDL at a solvent density of 1.019 g/mL. The infranatant, containing LDL and HDL, was brought to the original volume. The free cholesterol content of the solution was determined before and after precipitation of LDL with dextran sulfate and $MgCl_2$ (Kostner, 1976). LDL-free cholesterol, calculated by the difference between the original and supernatant-free cholesterol concentrations, was 25 ± 3 mg/dL. The rate of esterification of cholesterol by LCAT in plasma was determined as the rate of decrease of plasma free cholesterol as a function of time (Fielding & Fielding, 1981a) at 22 and 37 °C, and was linear with time over at least 2 h in each case. The rate of free cholesterol esterified was 11.5 ± 1.8 and 2.3 ± 0.6 μg (mL of plasma)$^{-1}$ h^{-1} at 37 and 22 °C, respectively.

Kinetic Analysis. First-order constants for the rate of transfer of free cholesterol label from LDL to HDL were determined from the plot of ln $(1 - x/x_\infty)$ vs time where x was the fraction of label transferred at time t and x_∞ was the distribution at infinite time, i.e., the proportion of total plasma free cholesterol in HDL. k was calculated from the slope of ln $(1 - x/x_\infty)$ vs t as $k = -(\text{slope } x/x_\infty)$ by least-squares analysis. The half-time for exchange ($t_{1/2}$) was obtained as ln $(2/k)$. Individual free cholesterol fluxes (moles per minute) were calculated as $k \times$ moles. Activation energy was calculated from the Arrhenius plot of ln k vs the reciprocal of the absolute temperature (degrees kelvin) using the temperature range 12–37 °C (283–310 K). Analogous calculations were made for the transfer of free cholesterol label within HDL subfractions separated by nondenaturing gel electrophoresis as described above.

Results

Comparison of Cellular and LDL Cholesterol Fluxes to HDL. When [^{3}H]cholesterol-labeled LDL tracer was incubated at 37 °C with native plasma in the presence of unlabeled cell monolayers, there was a rapid movement of labeled cholesterol out of LDL into HDL as a function of time (Figure 3). The transfer of LDL cholesterol to α-migrating HDL followed first-order kinetics with a mean rate constant (at 37 °C) of 0.0134 ± 0.002 min^{-1} (Table I). Radioactivity in the washed cell monolayer was determined after incubation. The cells contained <5% of HDL label. As the mean plasma LDL free cholesterol concentration in these experiments was 252 ± 26 μg/mL of plasma, the mean LDL free cholesterol flux to HDL was 3.4 ± 0.5 μg cholesterol min^{-1} (mL of plasma)$^{-1}$. The calculated $t_{1/2}$ (0.86 h) was very similar to the value (0.75 h) reported for the diffusional transfer of cholesterol in mixtures of centrifugally isolated LDL and HDL (Lund-Katz et al., 1982).

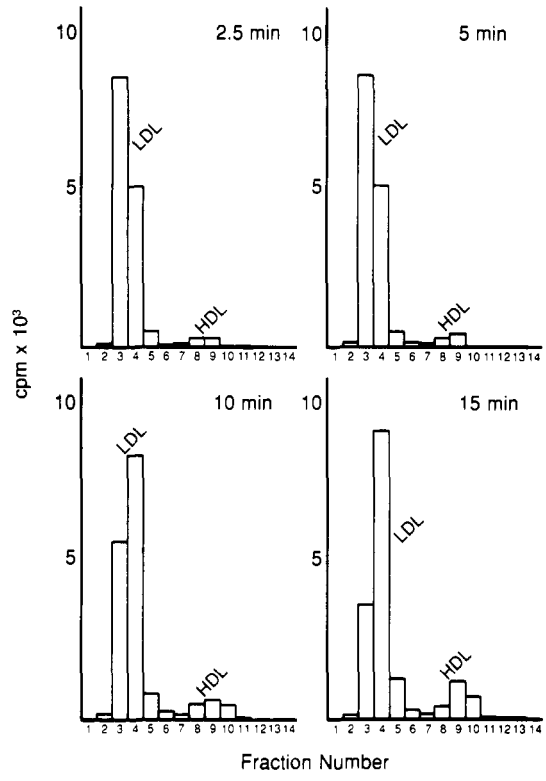

FIGURE 3: Transfer of LDL [^{3}H]cholesterol to HDL as a function of time determined by agarose gel electrophoresis. Native plasma was labeled with tracer [^{3}H]cholesterol LDL as described under Experimental Procedures and then incubated for the indicated time at 37 °C. After being cooled in ice–water, the plasma was fractionated by electrophoresis, and the label contained in 0.5-cm fractions was determined by liquid scintillation spectrometry.

Table I: Kinetics of Cholesterol Flux between LDL and HDL in Native Plasma[a]

donor	acceptor	temp °C	k (×10^3 min^{-1})	$t_{1/2}$ h	flux to HDL (μg min^{-1})
LDL	HDL	37	13.4 ± 2.0	0.86	3.4 ± 0.5
LDL	HDL	22	3.5 ± 0.3	3.30	0.9 ± 0.1
LDL	HDL	12	0.8 ± 0.2	14.4	0.2 ± 0.1

[a] First-order rate constants (k) and $t_{1/2}$ values were calculated from the rate of transfer of label from LDL to HDL as described under Experimental Procedures. Flux rates to HDL are calculated from the mean LDL free cholesterol content of plasma used in this study (252 μg mL^{-1}).

Further information on the mechanism of LDL-to-HDL cholesterol transfer was obtained from the temperature dependence of the rate constant k. Its calculated activation energy, calculated from the Arrhenius plot of ln k vs $1/T$, was 18.0 kcal/mol. This value is comparable to that determined experimentally (17 ± 1 kcal/mol) for the flux between synthetic phospholipid vesicles (McLean & Phillips, 1981) or the value (19 ± 1 kcal/mol) determined for the exchange of free cholesterol between isolated LDL and HDL (Lund-Katz et al., 1982).

Molecular Properties of α-HDL Subfractions. It is well recognized that the size distribution of HDL is discontinuous. Major subfractions characterized as HDL_{2b}, HDL_{2a}, and HDL_3 in increasing order of density have been identified (Anderson et al., 1978). The same particles can also be separated by nondenaturing polyacrylamide gradient gel electrophoresis into fractions with different diameters. HDL_{2b} represents the largest, lipid-rich HDL, HDL_{2a} a fraction of

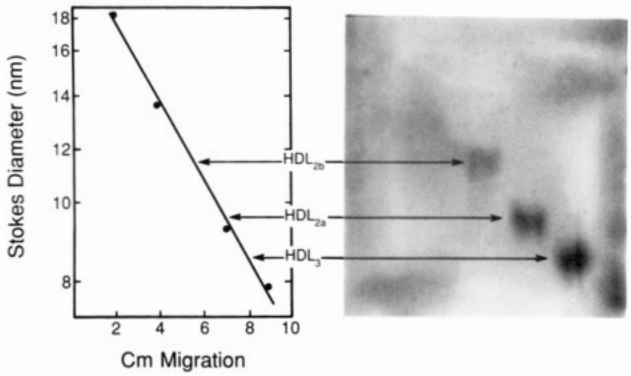

FIGURE 4: Stokes diameter of HDL_{2b}, HDL_{2a}, and HDL_3 determined by equilibrium nondenaturing polyacrylamide gradient gel electrophoresis. α-Migrating HDL fractions, eluted after two-dimensional electrophoresis, were characterized in a 3–24% polyacrylamide gel gradient. Thyroglobulin, apoferritin, amylase, and albumin protein standards were run simultaneously, and the slope of the correlation between the Stokes diameter and migration distance was determined by least-squares analysis from these standards. The migration rates and apparent Stokes radii of HDL_{2b}, HDL_{2a}, and HDL_3 are also shown.

Table II: Properties of α-Migrating HDL Subfractions Isolated by Nondenaturing Polyacrylamide Gel Electrophoresis[a]

fraction	Stokes diameter (nm)	apo A-I (%)	FC (%)	FC/apo A-I
HDL_{2b}	11.3 ± 0.3	17.9 ± 3.5	39.5 ± 15.0	2.22 ± 0.64
HDL_{2a}	9.4 ± 0.2	40.0 ± 4.5	50.4 ± 10.2	1.25 ± 0.18
HDL_3	8.4 ± 0.2	31.9 ± 1.8	5.9 ± 1.9	0.18 ± 0.06

[a] Stokes diameter was determined by equilibrium gradient gel electrophoresis as described under Experimental Procedures. The percent of total apo A-I in the combined α-migrating HDL fraction in these experiments was 89.7 ± 4.3%. Apo A-I in the combined pre-βHDL fractions was 10.1%. Similarly, α-migrating HDL free cholesterol was 95.8 ± 1.3% of the total HDL free cholesterol, with the balance in the total pre-βHDL fraction.

intermediate size and density, and HDL_3 the smallest HDL, relatively poor in lipid. To obtain further information on the early HDL acceptors of LDL-derived free cholesterol label, the gradient electrophoretic separation previously described was modified as described under Experimental Procedures and the major αHDL fractions recovered by elution. The molecular diameter and purity of the fractions identified in Figure 2 were determined by equilibrium gradient gel electrophoresis. Stokes diameters for the three fractions were 11.3, 9.4, and 8.4 nm (Figure 4), almost identical with those reported previously by Anderson et al. (1977) for centrifugal HDL_{2b}, HDL_{2a}, and HDL_3, respectively. These studies also demonstrated that well-purified fractions of αHDL were separated by the electrophoretic technique described here. As a further basis for comparison, the distribution of apo A-I and free cholesterol within these HDL subfractions was also determined (Table II). Apo A-I distribution was quantified from the distribution of ^{125}I-labeled second antibody following the reaction of the electrophoretically separated lipoproteins with anti-apo A-I antibody, as described under Experimental Procedures. Free cholesterol distribution at equilibrium within HDL was determined by incubating plasma (in the presence of DTNB to inhibit LCAT activity) for 60 min with ^{3}H-labeled LDL. As discussed below, this represents at least $10 \times t_{1/2}$ for the transfer within HDL.

The results are shown in Table II. The fraction of intermediate size (HDL_{2a}) contained the major part of both apo A-I and free cholesterol. The smallest αHDL particles (HDL_3) were relatively poor in free cholesterol compared to apo A-I content, while the cholesterol/apo A-I ratio was highest in HDL_{2b}.

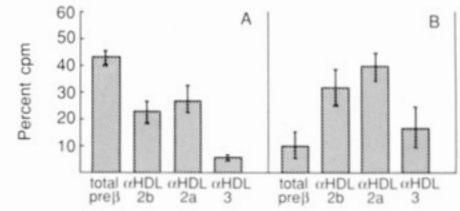

FIGURE 5: Distribution of cholesterol radiolabel between pre-βHDL, HDL_{2b}, HDL_{2a}, and HDL_3 following 1-min incubation with either ^{3}H-labeled cultured fibroblasts (left) or ^{3}H-labeled LDL (right). The pre-β label represents the sum of label in the three components of pre-βHDL shown in Figure 2.

Comparison of the Metabolism of Cell-Derived and LDL-Derived Free Cholesterol. Experiments were carried out to determine whether cholesterol from LDL (like cholesterol from cell membranes) used the pre-βHDL pathway described earlier (Castro & Fielding, 1988). Portions of native plasma were incubated (0.5–1.0 min) at 37 °C either with cell monolayers previously equilibrated with labeled cholesterol or (after mixing with labeled LDL) with unlabeled cell monolayers. The distribution of cholesterol radioactivity was determined following nondenaturing two-dimensional electrophoresis. As shown in Figure 5, 42.4 ± 4.6% of the free cholesterol radioactivity transferred from cell membranes was recovered in the pre-βfraction, comparable to the 50 ± 24% reported earlier in similar experiments and much greater than the proportion of free cholesterol recovered in the same fraction. On the other hand, with LDL-derived cholesterol, under the same conditions there was a much lower recovery of label (8.2 ± 5.0%) in pre-βHDL; that is, almost all was recovered in the total αHDL fraction. For both LDL-derived and cell-derived HDL, the greatest part of the label in αHDL was in the HDL_{2a} fraction. However, there was a 3–4-fold greater recovery of label in HDL_3 when the label was transferred from LDL than when it had been transferred from cell membranes. This probably relates (as discussed below) to the different sites of esterification of cell- and LDL-derived cholesterol by the LCAT reaction.

Two possibilities might explain this different distribution. Either LDL free cholesterol (unlike that from cell membranes) did not use the pre-βHDL pathway to a significant extent, or else, because the transfer of cholesterol from LDL was more rapid than from cell membranes, label had already largely equilibrated between the pre-β and αHDL fractions after 0.5–1.0 min at 37 °C. If the second hypothesis were correct, reduction of the incubation temperature should result in an increased recovery of LDL-derived cholesterol label in pre-βHDL. To test this, the 37 °C distribution experiment shown in Figure 5 was carried out at 12 and 22 °C, conditions which reduce the rate constant for transfer up to 20-fold (Table I), such that at 12 °C, the first-order rate constant for efflux from LDL (0.8×10^{-3} min^{-1}) is similar to that from cultured cell monolayers (Fielding & Fielding, 1981). At 22 °C, label in pre-βHDL was 4.8 ± 1.6%. At 12 °C, 5.5 ± 2.2% of the total label was in pre-βHDL compared with 8.2 ± 5.0% at 37 °C. These data indicate that even at low transfer rates, LDL cholesterol label is not concentrated to a significant extent in pre-βHDL. This suggests that fundamentally different pathways are utilized in the early metabolism of LDL-derived and cell-derived cholesterol.

Kinetics of Free Cholesterol Radioactivity within HDL. To obtain further information on the metabolism of LDL-derived cholesterol within HDL, the [^{3}H]cholesterol content of the

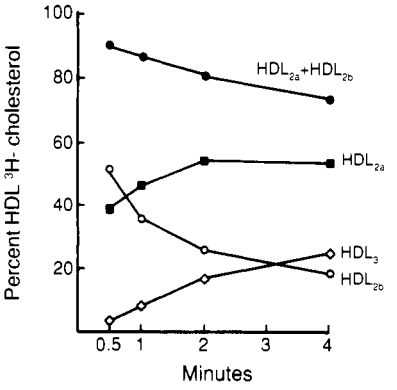

FIGURE 6: Distribution of cholesterol radiolabel between α-migrating HDL subfractions as a function of time at 22 °C. After addition of tracer [^{3}H]cholesterol-labeled LDL, plasma was incubated for the time indicated, and after cooling to 0 °C, it was fractionated by two-dimensional electrophoresis as described under Experimental Procedures. Open circles, label in HDL_{2b}; closed squares, label in HDL_{2a}; closed circles, total label in HDL_{2b} + HDL_{2a}; open squares, label in HDL_3.

different αHDL fractions was determined at 22 °C.

As shown in Figure 6, there were significant changes in the distribution of [^{3}H]cholesterol within HDL as a function of time. At 0.5 min, there was little or no label in HDL_3, while HDL_2 contained the major part of the radioactivity. As incubation continued, an equilibrium was approached in which the label in HDL_3 represented about 25% of the total flux. At the same time, label in HDL_{2b} was reduced to about 20%. When these data were expressed in terms of first-order rate constants for the transfer of label from HDL_{2b}, and for the transfer of label from HDL_{2a}, linear plots for $\ln (1 - x/x_\infty)$ vs t over a time course of 0.5–4 min were obtained in each case. The extrapolation of these plots to zero time passed through $\ln (1 - x/x_\infty) = 0$, consistent with the concept that most or all of HDL label originated in HDL_{2b} and that there was little direct transfer from LDL to HDL_3. This suggests that the label in HDL_3 was derived during incubation from HDL_{2b} and HDL_{2a}. Extrapolation of these data suggested that essentially the whole label appearing in α-migrating HDL was initially transferred to the largest (HDL_{2b}) fraction and that label in HDL_{2a} and finally in HDL_3 was derived by transfer from HDL_{2b}. The calculated first-order rate constant at 22 °C for the proportional decrease of LDL-derived ^{3}H radioactivity in HDL_{2b} was 0.16 min^{-1}, and that for the appearance of label in HDL_3 was 0.07 min^{-1}. The mean pool sizes of HDL_{2b} and HDL_{2a} were 23 and 61 μg of cholesterol/mL, respectively. The flux rate out of HDL_{2b} was therefore $0.16 \times 23 = 3.7$ $\mu g\ mL^{-1}\ min^{-1}$, while that from HDL_{2a} to HDL_3 was $0.07 \times 61 = 4.2$ $\mu g\ mL^{-1}\ min^{-1}$. Both of these rates are greater (at 22 °C) than the flux from LDL to HDL of 0.9 $\mu g\ mL^{-1}\ min^{-1}$, suggesting there is substantial recycling of free cholesterol between HDL subspecies.

Evidence for a Cholesterol Gradient within HDL. The major factor modifying plasma free cholesterol levels is the activity of LCAT as it converts diffusible free cholesterol in HDL to its insoluble ester form (Fielding, 1984). An indication of the role of the LCAT reaction in the transfer of cholesterol label within HDL was obtained when the equilibrium distribution of label within the major HDL subfractions in the presence and absence of the LCAT inhibitor DTNB was compared (Table III). LCAT significantly reduced the level of label in HDL_{2b} while increasing it by about the same proportion in HDL_3. These data indicate that the action of LCAT modifies the equilibrium of LDL-derived free cholesterol between HDL_{2b} and HDL_3. It is of interest that

Table III: Equilibrium Distribution of HDL Subfraction Free Cholesterol in the Presence and Absence of LCAT Activity[a]

fraction	fraction of total label from LDL		fraction of total label from cells
	-DTNB	+DTNB	
HDL_{2b}	0.20 ± 0.07	0.39 ± 0.15	0.41 ± 0.05
HDL_{2a}	0.53 ± 0.06	0.50 ± 0.10	0.50 ± 0.09
HDL_3	0.25 ± 0.08	0.06 ± 0.02	0.09 ± 0.04

[a] Values given are the proportion of total αHDL label from LDL or cultured cell monolayers labeled with [^{3}H]cholesterol. Distributions were obtained after 4 min at 37 °C.

the distribution of free cholesterol label derived from cell membranes when LCAT is active is similar to that when the label is LDL-derived and LCAT is inhibited (Table III, columns 2 and 3). This suggests that the metabolism of cell-derived free cholesterol (unlike that derived from LDL) is not closely coupled to the activity of LCAT in the α-migrating HDL fraction. This result is consistent with the concept (Francone et al., 1989) that a major part of cell-derived cholesterol is metabolized through an alternative (pre-βHDL) pathway.

Discussion

LDL has been previously identified as the major source of lipoprotein-free cholesterol substrate for LCAT activity in normal human plasma (Fielding & Fielding, 1981a; Park et al., 1983). However, almost all cholesterol esterification in human plasma occurs within HDL (Francone et al., 1989). LCAT activity must therefore involve the transfer of LDL cholesterol to HDL. The present study deals with the mechanism of this reaction.

In spite of the complex organization of lipoproteins (particularly HDL) in native plasma, the transfer of free cholesterol from LDL to HDL has thermodynamic characteristics numerically compatible with those expected for simple diffusion. The first-order transfer rate (0.0134 min^{-1} at 37 °C) in native plasma is similar to that established between isolated LDL and other lipoproteins (Lund-Katz et al., 1986). The activation energy of cholesterol transfer from LDL (18 kcal/mol) is also very similar to the theoretical value calculated from the diffusion coefficient of cholesterol. It is also similar to that obtained for transfer between several synthetic vesicle systems [for a review, see Fielding (1984)]. However, the selectivity of acceptor shown in the present research for HDL_{2b}, and for pre-βHDL in an earlier study (Castro et al., 1988), suggests a more complex mechanism possibly involving both an activation step [perhaps identical kinetically with the desorption proposed by McLean and Phillips (1981)] and a collision step in which the selectivity demonstrated in this study could be expressed (Steck et al., 1988). In any event, it seems clear that cholesterol kinetics in native plasma are both nonequilibrium and selective.

Cholesterol transfer from a variety of normal cell membranes to plasma lipoproteins, like that from LDL, appears to be driven by LCAT activity (Ray et al., 1980; Fielding & Fielding, 1981; Davis et al., 1982; Chollet et al., 1986). Since the concentration of LDL free cholesterol in plasma is about 250 $\mu g\ mL^{-1}$ in these studies, this pathway generates a flux of about 3–4 μg of free cholesterol $mL^{-1}\ min^{-1}$ from LDL to HDL at 37 °C. The corresponding flux at 22 °C was 0.9 $\mu g\ mL^{-1}\ min^{-1}$. This is in both cases at least 10-fold greater than the requirement of cholesterol for the esterification rates via the LCAT reaction under both conditions reported above. However, since only a fraction of αHDL particles contain bound LCAT, much of this flux may be ineffectual enzy-

matically. This situation appears to be quite different from that observed previously with cell-derived cholesterol where pre-βHDL contained about 35% of total LCAT activity vs only 4–5% of HDL-free cholesterol (Francone et al., 1989).

As previously reported, cell-derived cholesterol was metabolized mainly via a minor pre-β-migrating HDL fraction which was rapidly converted, probably by polymerization, into a high molecular weight complex containing a high concentration of LCAT molecules compared to the rest of HDL (Francone et al., 1989). The preference of cell-derived cholesterol for the pre-β pathway is confirmed in the present study. LDL-derived free cholesterol is evidently metabolized through a distinct pathway involving the α-migrating HDL fraction. The present study shows for the first time that cell-derived and LDL-derived free cholesterol are metabolized via two different lipoprotein pathways, providing further evidence for an effective compartmentation of free cholesterol in native plasma.

This study also demonstrates marked functional heterogeneity within the αHDL fraction. In terms of the early recovery of LDL cholesterol label, the major part of early labeling is associated with the largest (HDL_{2b}) fraction, even though this contains a relatively small proportion (about 20%) of the total HDL free cholesterol. As labeling in this fraction decreases with time toward its equilibrium, the label appears in HDL_{2a} and finally in the HDL_3 fraction. There appears to be recycling of cholesterol between the α subfractions. The molecular basis of this observed transfer is not yet clear, although it may involve protein-catalyzed free cholesterol transfer such as that recently described and dependent on apolipoprotein A-II (Coughlin et al., 1988). It may be important that apo A-II is present in all αHDL fractions but is completely absent from pre-βHDL (Castro & Fielding, 1988). Overall, the effect of this HDL speciation is to maintain a disproportionately high concentration of labeled free sterol in HDL_3 (Table III). As this effect is lost when LCAT is inhibited, it seems likely that the enzyme, by utilizing free cholesterol mainly on HDL_3, drives a chemical potential gradient that increases the supply of substrate. Consistent with this hypothesis, HDL_3 appears to be the most effective major HDL substrate for the LCAT reaction (Fielding & Fielding, 1971; Jahani & Lacko, 1982).

In summary, this research provides further evidence for the compartmentation of free cholesterol within HDL and indicates a mechanism by which cell and lipoprotein cholesterol could be individually packaged in lipoprotein form for later catabolism.

Registry No. Cholesterol, 57-88-5; lecithin–cholesterol acyltransferase, 9031-14-5.

References

Allain, C. C., Poon, C. S. G., Chan, W., Richmond, W., & Fu, P. C. (1974) *Clin. Chem. 20*, 470–475.

Anderson, D. W., Nichols, A. V., Forte, T. M., & Lindgren, F. T. (1977) *Biochim. Biophys. Acta 493*, 55–68.

Anderson, D. W., Nichols, A. V., Pan, S. S., & Lindgren, F. T. (1978) *Atherosclerosis 29*, 161–179.

Bucolo, G., & David, H. (1973) *Clin. Chem. 19*, 476–482.

Castro, G. R., & Fielding, C. J. (1988) *Biochemistry 27*, 25–29.

Chollet, F., Perret, B. P., Chap, H., & Douste-Blazy, L. (1986) *Biochim. Biophys. Acta 875*, 135–146.

Coughlin, B. A., Kezdy, F. J., Heinrickson, R. L., & Meredith, S. C. (1988) *Arteriosclerosis 8*, 594a.

Davis, R. A., Helgerud, P., Dueland, S., & Drevon, C. A. (1982) *Biochim. Biophys. Acta 689*, 410–414.

Fielding, C. J. (1984) *J. Lipid Res. 25*, 1624–1628.

Fielding, C. J. (1990) in *Advances in Cholesterol Research* (Esfahani, M., & Swaney, J., Eds.) pp 270–314, Telford Press, Caldwell, NJ.

Fielding, C. J., & Fielding, P. E. (1971) *FEBS Lett. 15*, 355–358.

Fielding, C. J., & Fielding, P. E. (1981a) *J. Biol. Chem. 256*, 2102–2104.

Fielding, C. J., & Fielding, P. E. (1981b) *Proc. Natl. Acad. Sci. U.S.A. 78*, 3911–3914.

Fielding, P. E., & Fielding, C. J. (1986) *J. Biol. Chem. 261*, 5232–5236.

Fielding, P. E., Davison, P. M., Karasek, M. A., & Fielding, C. J. (1982) *J. Cell Biol. 94*, 350–354.

Francone, O. L., Gurakar, A., & Fielding, C. J. (1989) *J. Biol. Chem. 264*, 7066–7072.

Ishida, B. Y., Frohlich, J., & Fielding, C. J. (1987) *J. Lipid Res. 28*, 778–786.

Jahani, M., & Lacko, A. D. (1981) *J. Lipid Res. 22*, 1102–1110.

Kostner, G. M. (1976) *Clin. Chem. 22*, 695.

Lund-Katz, S., Hammerschlag, B., & Phillips, M. C. (1982) *Biochemistry 21*, 2964–2969.

McLean, L. R., & Phillips, M. C. (1981) *Biochemistry 20*, 2893–2900.

Park, M.-S. C., Kudchodkar, B. J., Frohlich, J., Pritchard, H., & Lacko, A. G. (1987) *Arch. Biochem. Biophys. 258*, 545–554.

Porath, J. R., Axen, R., & Ernback, S. (1967) *Nature (London) 215*, 1491–1492.

Ray, E., Bellini, F., Stoudt, G., Hemperley, S., & Rothblat, G. (1980) *Biochim. Biophys. Acta 617*, 318–334.

Rodbard, D., Kapadias, G., & Chrambach, A. (1971) *Anal. Biochem. 40*, 135–157.

Steck, T. L., Kezdy, F. J., & Lange, Y. (1988) *J. Biol. Chem. 263*, 13023–13031.

Stokke, K. T., & Norum, K. R. (1972) *Scand. J. Clin. Lab. Invest. 27*, 21–27.